

Article

Real-life/real-time elderly fall detection with a triaxial accelerometer

A. Sucerquia ¹ , J.D. López ^{2,†}  and J.F. Vargas-Bonilla ^{2,‡} 

¹ Facultad de Ingeniería, Institución Universitaria ITM, Medellín, Colombia (e-mail luzsucerquia@itm.edu.co)

² SISTEMIC, Facultad de Ingeniería, Universidad de Antioquia UDEA, Calle 70 No. 52-21, Tel.: +57-4-2198561, Medellín, Colombia (e-mail [†]josedavid@udea.edu.co, [‡]jesus.vargas@udea.edu.co)

* Correspondence: luzsucerquia@itm.edu.co; Tel.: +57-460-0727 ext. 5586

Abstract: The consequences of a fall on an elderly person can be reduced if the accident is attended by medical personnel within the first hour. Independent elderly people use to stay alone for long periods of time, being in more risk if they suffer a fall. The literature offers several approaches for detecting falls with embedded devices or smartphones using a triaxial accelerometer. Most of these approaches were not tested with the target population, or are not feasible to be implemented in real-life conditions. In this work, we propose a fall detection methodology based on a non-linear classification feature and a Kalman filter with a periodicity detector to reduce the false positive rate. This methodology requires a sampling rate of only 25 Hz; it does not require large computations or memory and it is robust among devices. We test our approach with the SisFall dataset achieving 99.4 % of accuracy. Then, we validate it with a new round of simulated activities with young adults and an elderly person. Finally, we give the devices to three elderly persons for full-day validations. They continued with their normal life and the devices behaved as expected.

Keywords: Triaxial accelerometer; Wearable devices; Fall detection; Mobile health-care; SisFall; Kalman filter.

1. Introduction

At least one third of elderly people suffers a fall per year and the probability of falling increases with age and previous falls [1–4]. The consequences of a fall can be reduced if the person is attended by medical services within an hour from the accident [5–7]. This timing is feasible with institutionalized elderly people, but healthy independent elderly people use to stay alone for long periods of time increasing their risk of aggravating the injuries in case of an accident. Nowadays, authors focus on developing automatic fall detection systems, which generate an alarm in case of an event, but they still present high error rates in real-life conditions (see [7–10] for reviews on the field). In this paper, we tackle this issue with a novel fall detection methodology tested in real-life situations with the target population, using a simple to implement triaxial-accelerometer-based embedded device.

Detecting falls with a triaxial accelerometer is commonly divided in three stages: pre-processing, feature extraction, and classification. The preprocessing can be as simple as a low-pass filter [11], but it mainly depends on the selected feature extraction. In this sense, there is a wide amount of features available in the literature, such as acceleration peaks, variance, angles, etc. (see [9, Table 4] for a complete list). These features transform the acceleration signal in order to better discriminate between falls and activities of daily living (ADL). Regarding classification, threshold based detection is still the most opted choice over machine learning alternatives, mainly because the latter are impractical for real-time implementation. Habib et al. [10] show various examples of SVM approaches consuming the battery in few hours and Igual et al. [12] concluded that these approaches are highly dependent on the acquisition device used.

A common problem with approaches proposed in the literature is that most of them were tested with young adults under controlled conditions [9, Table 5]. Moreover, previous works demonstrated

37 that the accuracy of these approaches is significantly reduced when tested on institutionalized [13]
38 and independent [11] elderly people. The main reason authors have for not testing with the target
39 population is the lack of appropriate public datasets and the difficulty of acquiring real falls with
40 elderly people [9,11,13]. In order to tackle these issues, we recently released the SisFall dataset [11], a
41 fall and movement dataset acquired with a triaxial accelerometer mounted on an embedded device
42 attached to the waist (see [14] for implementation details).

43 In [11], we demonstrated that most failures in fall detection are focused on a few activities. Most
44 of these activities coincide in periodic waveforms (from walk and jog) and high peak acceleration
45 ADL (e.g., jump). There are previous approaches in the literature for detecting jog and walk with
46 accelerometers. Cola et al. [15] detected gait deviation as a fall-risk feature. Oner et al. [16] used the
47 peaks of the acceleration signal measured with a smartphone to detect steps and subsequently the
48 kind of activity based on the period between steps. Wundersitz et al. [17] did it with an embedded
49 device. Other authors used more elaborated metrics but all peak based. Clements et al. [18] computed
50 principal components of the Fast Fourier Transform (FFT), to cite an example. In contrast, we previously
51 developed a more stable gait detector based on wavelet or auto-correlation indistinctly [19]. However,
52 it was too computationally intensive for real-life implementation in an embedded device.

53 In this work, we present a Kalman-filter-based fall detection algorithm that additionally detects
54 gait as a feature to avoid false positives. The fall detection feature is a novel non-linear metric based
55 on two widely used features: the sum vector magnitude and the standard deviation magnitude. The
56 Kalman filter is a well-known optimal estimator [20] widely used in several research fields. The
57 Kalman filter is Markovian (avoiding large memory storage) and linear (simple computations for
58 lower energy consumption). Here, we use it as an input to the non-linear feature by determining
59 the orientation of the subject: jogging activities may lead to high accelerations, but the absence of
60 inclination implies that the subject is not falling. We additionally use the Kalman filter to smooth gait
61 patterns (as sinusoidal-shape waveforms) in order to feed our gait detector.

62 The Kalman filter has been previously used to identify movements of interest with accelerometers.
63 Bagalà et al. [21] used it to determine the lie-to-sit-to-stand-to-walk states, which are commonly
64 used to measure the risk of falling in elderly people (with the Berg Balance Scale –BBS– for example
65 [22]). There, the authors used an extended Kalman filter to determine the orientation of the device.
66 Otebolaku et al. [23] proposed a novel user context recognition using a smartphone. In their work, the
67 Kalman filter was used to obtain the orientation of the device based on its multiple sensors (not only
68 the accelerometer). But the authors did not specify how they did it. Finally, Novak et al. [24] used a
69 multiple sensors system to determine gait initiation and termination. In their work, the Kalman filter
70 was used again to obtain the orientation of the device.

71 Aforementioned works coincide in their objective with the Kalman filter (identifying locomotion
72 activities), but they differ on the way it was implemented and none of them was interested in detecting
73 falls. Some other authors have used the Kalman filter as part of their fall detection algorithms [25–29].
74 All of them used the triaxial accelerometer together with other sensors (a gyroscope in all cases and a
75 magnetometer in one case). In these works, the Kalman filter was used for de-noising, data fusion,
76 and to obtain the device angle. The main difference among these works is the classification strategy:
77 threshold, SVM, neural networks, or Bayesian classifier.

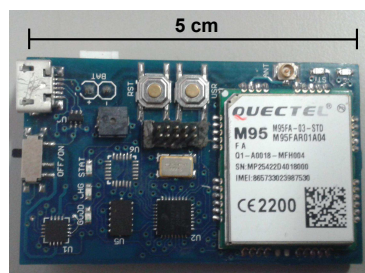
78 Our approach differs from these previous works in several key features: (i) one of our main
79 purposes is to extend the battery life of the device. Following this, we only use one triaxial
80 accelerometer. We discarded to use a gyroscope because it typically consumes more than ten times
81 more current than the accelerometer (40 – 145 μA for the ADXL345 that we selected, compared to
82 hundreds of μA to some mA for a gyroscope). (ii) We present a novel non-linear classification feature
83 that allows us to obtain high accuracy values with a simple thresholding approach. (iii) We include a
84 gait detector to discard false positives caused by high acceleration periodic activities. (iv) We validate
85 on real-time and under uncontrolled conditions with the target population.

86 This paper continues as follows: In Sections 2 and 3, we present the dataset used and explain the
 87 proposed approach. In Section 4, we present the overall results with controlled activities and falls (in
 88 simulation and implemented on an embedded device); we perform an individual activity analysis;
 89 and we show an on-line validation, where three elderly voluntaries carried an embedded device for
 90 several days each. Finally, we discuss our findings in Section 5.

91 2. Materials

92 We recently published a dataset with falls and ADL acquired with accelerometer (SisFall: Sistic
 93 research group fall and movement dataset [11]). Here we use this dataset to train and test the proposed
 94 approach. It was generated with 38 participants divided in elderly people and young adults. Twenty
 95 three young adults performed five repetitions of 19 ADL and 15 fall types, while 14 participants over
 96 62 years old performed 15 ADL. One additional participant, a 60 years old participant, performed
 97 both ADL and falls. The dataset was acquired with a self-developed embedded device attached to the
 98 waist [14]. The embedded device was based on a Kinets MKL25Z128VLK4 microcontroller with an
 99 ADXL345 accelerometer. The accelerometer was configured for ± 16 G, 13 bits of ADC, and a sampling
 100 rate of 200 Hz.

101 A second device was developed for validating our methodology (Figure 1). This device consisted
 102 of the same microcontroller and sensor used for SisFall, but it included a GPRS transmitter (to send
 103 short text messages –SMS) that was activated if a fall was detected. As we did with the first device, it
 104 was fixed with a homemade belt (see the supplementary videos of [11]) to guarantee that it did not
 105 move relative to the subject. Neither it required to be completely vertical nor to have an additional
 106 calibration once the subject wore it.



(a) Device used for implementing and testing the proposed approach



(b) Participants using the device

Figure 1. Validation device. (a) With similar characteristics of the device used in [11], this one included a GPRS module able to send text messages in case of alarm. (b) Note how the elderly participants did not wear the device exactly on the expected position/orientation (The photos show positions observed at the end of uncontrolled recordings).

107 Two additional validation tests were performed with this device:

- 108 • Individual activities: Six young adults (subjects SA03, SA04, SA05, SA06, SA09, SA21) and one
 109 elderly person (subject SE06) performed again three trials of all activities in SisFall (except D17,
 110 getting in and out of a car, due to logistic issues).
- 111 • On-line uncontrolled tests: We gave the device to three elderly participants that were not part
 112 of SisFall dataset. They were independent and healthy. Table 1 shows their gender, age, height
 113 and weight. The subjects used the device permanently for several days, except during sleep and
 114 shower (as the device is not water-proof yet). We used three devices to guarantee the integrity of
 115 the system.

Table 1. Gender, age, height and weight of the on-line test participants.

Code	Gender	Age	Height [m]	Weight [kg]
SM01	Female	61	1.56	54
SM02	Female	70	1.46	56
SM03	Male	81	1.62	68

116 All activities performed by the participants were approved by the Bio-ethics Committee of the
 117 Medicine Faculty, Universidad de Antioquia UDEA (Medellín, Colombia). Additionally, all participants
 118 were evaluated by a sports specialized physician.

119 3. Methods

120 Figure 2 shows a schematics of the proposed approach. It includes bias variations of the signal
 121 together with acceleration peaks. This increases the robustness of the feature extraction and allows
 122 simpler classifiers. The proposed methodology consists of four stages: Preprocessing, feature extraction,
 123 classification, and periodic activity detection. For each time sample k , the raw acceleration data $\vec{a}[k]$
 124 is initially low-pass filtered. Then, it splits into bias removal and Kalman filtering, which feeds
 125 both features J_1 and J_2 respectively (see Eqs. (8) and (9) below). A threshold-based classification
 126 is performed over a non-linear indirect feature. If the resultant value crosses the threshold, the periodicity
 127 of the signal (extracted from the Kalman filter and a zero-crossing algorithm) is analyzed in order to
 128 determine if it is a false fall alert or if indeed the alarm should be turned on. This methodology is
 129 explained in the following section.

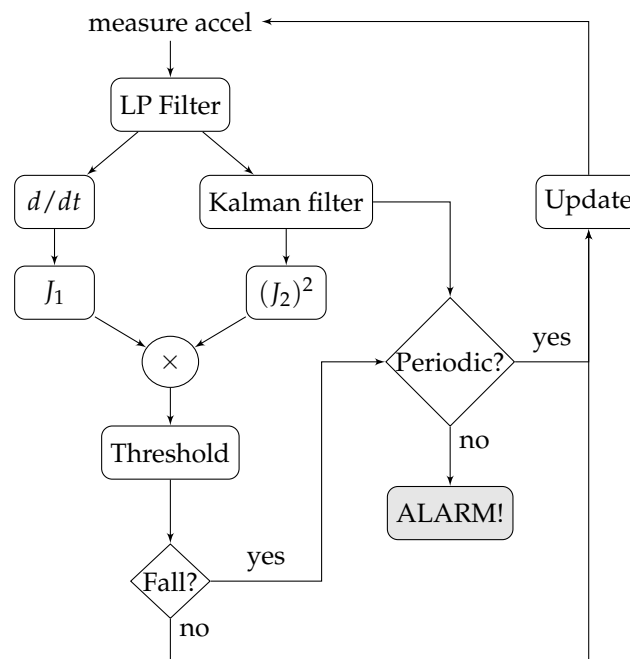


Figure 2. Proposed methodology. It is based on a non-linear feature that allows detecting falls with a simple threshold based detector. Then, false positives are discarded if a periodic activity is detected after the fall.

130 3.1. Preprocessing and periodicity detector

131 The same 4-th order IIR low-pass Butterworth filter with a cut-off frequency of 5 Hz proposed
 132 in [11] was used in this work. This filter was selected because: (i) It can be implemented in simple

133 embedded devices; (ii) It does not require large computations in software; and (iii) an increase in the
 134 order or in the cut-off frequency does not improve the accuracy; consequently, it does not require
 135 higher sampling frequencies. Filtered data are then bias removed with a simple differentiation of
 136 consecutive samples, as it is needed to compute the static feature (J_1). SisFall dataset was initially
 137 acquired at 200 Hz; however, the proposed methodology only requires 25 Hz to feed the filter. Then,
 138 all results presented here correspond to the proper downsampled signals.

139 The second feature (J_2) is computed over the bias level, which is obtained with a Kalman filter. A
 140 Kalman filter [20] is an optimal quadratic estimator able to recover hidden states of a state-space model.
 141 It was used here with two purposes: to recover the bias-level variation and to find the periodicity
 142 of the signal. To achieve this, the Kalman filter acts as a set of adaptive FIR filters with the objective
 143 of estimating parameters/states of a dynamical system. As any Luemberger-type estimator [30], the
 144 estimation is improved by working in closed loop, which allows updating the input and using the
 145 historic values collected on the Markovian process. Additionally, being a multivariable estimator, the
 146 Kalman filter includes both the variance and covariance of the signal to filter (something unfeasible
 147 with FIR filters). Finally, as an adaptive filter, it has more immunity to model uncertainty, noise, and
 148 perturbations than FIR filters (it is optimal on the quadratic mean, and it is robust).

149 Let us define the filtered acceleration data as $\vec{a}[k] = [a_x, a_y, a_z]^T \in \mathfrak{R}^{3 \times 1}$ for time instant k , where
 150 a_x , a_y , and a_z are single samples of raw acceleration (in practice, it comes in bits, as acquired by the
 151 ADC of the device). These data feed the following autonomous state-space model:

$$\begin{aligned}\vec{x}[k] &= A\vec{x}[k-1] + \eta \\ \vec{y}[k] &= C\vec{x}[k] + \epsilon\end{aligned}\quad (1)$$

152 where the first three states of $\vec{x} \in \mathfrak{R}^{4 \times 1}$ are used for classification and the fourth state x_4 removes
 153 peaks from periodic signals (see Figure 3, example with activity F05: jog, trip, and fall). As this
 154 Kalman filter is exclusively used for smoothing (and not for feature extraction or classification), the
 155 state transition $A \in \mathfrak{R}^{4 \times 4}$ and output $C \in \mathfrak{R}^{4 \times 4}$ matrices are identity matrices. Finally, the output
 156 is defined as $\vec{y} = [a_x, a_y, a_z, a_y - b_{a_y}]^T \in \mathfrak{R}^{4 \times 1}$, where the first three terms are the low-pass filtered
 157 acceleration data in the three axis and the fourth output is the acceleration on vertical axis minus its
 158 current bias b_{a_y} . The vertical bias $b_{a_y}[k]$ is dynamically updated with a sliding window of 1 s over the
 159 mean of the output of the Kalman filter. x_4 provides a zero-bias sinusoidal-shape waveform when
 160 the acceleration comes from periodic activities (walk, jog, going-up stairs, etc.). The period of this
 161 signal can be detected counting zero-crossings (changes of sign) and dividing by two over a given time
 162 window.

163 This state-space model is affected by Gaussian measurement noise $\epsilon = \mathcal{N}(0, R)$, and Gaussian
 164 state uncertainty $\eta = \mathcal{N}(0, Q)$. The objective of the Kalman filter is to minimize the variance of the
 165 states $P \in \mathfrak{R}^{4 \times 4}$, considering them as random variables with a Gaussian distribution: $\vec{x} = \mathcal{N}(\bar{x}, P)$.

166 The Kalman filter consists of five equations divided in two stages. The prediction stage of the
 167 Kalman filter predicts the current value of the states and their variance solely based on their previous
 168 values:

$$\vec{x}[k]^- = A\vec{x}[k-1] \quad (2)$$

$$P[k]^- = AP[k-1]A^T + Q \quad (3)$$

169 Both $\vec{x}[k]^-$ and $P[k]^-$ are intermediate values that must be corrected based on current data values:

$$G[k] = CP[k](CP[k]^{-1}C^T + R)^{-1} \quad (4)$$

$$\bar{x}[k] = \bar{x}[k]^{-} + G[k](\bar{y}[k] - C\bar{x}[k]^{-}) \quad (5)$$

$$P[k] = (I_4 - G[k]^T C)P[k]^{-} \quad (6)$$

170 where $I_4 \in \mathbb{R}^{4 \times 4}$ is a (4×4) identity matrix.

171 This strategy only requires to sintonize two parameters to set-up the Kalman filter: the variance
 172 matrices Q and R . There are not rules to determine their values, but specifically for this problem they
 173 are not difficult to define. Both are usually diagonal (no interaction among states), large values of Q
 174 and R tend to the original data: $\bar{x} \approx \bar{y}$, and they are also complementary, i.e., the states are flatten
 175 when reducing any of them. As shown in Figure 3 (Second and Third panels), the first three states are
 176 flat (inclination of the subject) and the fourth one seeks for periodic (sinusoidal shape) waveforms.

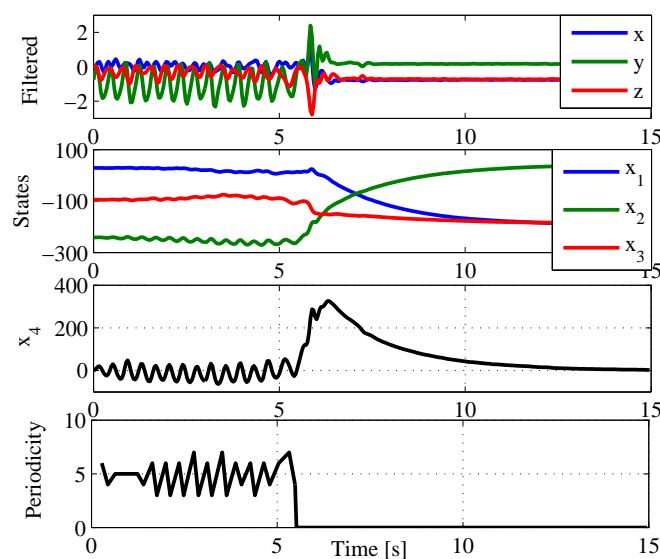


Figure 3. Kalman filtering. (Top panel) Reference filtered acceleration data (Activity F05 of SisFall: jog, trip, and fall) in gravities [G]. (Second panel) First three states of the Kalman filter. The filter estimates the bias-level variations of the signal. (Third panel) The fourth state of the Kalman filter recovers a quasi sinusoidal signal during the first 6 s. Its objective is to dynamically remove bias to allow posterior zero crossing detection. (Bottom panel) Periodicity detector. The first 6 s the subject is jogging with a period of 10 time samples (half zero crossings); when the subject suffers a fall it stops detecting periodicity too.

177 The states can be initialized with zero values, and $P[0] = Q$, i.e., selecting uninformative priors.
 178 However, for faster convergence $x_2[0]$ and $b_{a_y}[0]$ can be initialized with -1 G (approx. -258 in bytes for
 179 the device configuration used here), which is the initial condition of the accelerometer in our device.
 180 Q and R can be computed with a simple heuristic process: Using a walk and fall file for testing, (i)
 181 Initialize Q and R with identity matrices; then, (ii) for the first three states (first three diagonal values of
 182 Q and R) start an iterative process by reducing by 10 the standard deviation (square of each diagonal
 183 value) of Q and then doing the same with R , until the states start looking flat. A good fit can be done
 184 by reducing the scale to 5 and then to 2; although these matrices are poorly sensitive, i.e., the algorithm
 185 can work with approximate values. Finally, (iii) for the fourth state reduce Q and R (as in the previous
 186 step) until x_4 shows a sinusoidal shape in periodic activities (walk and jog). The objective is to clean
 187 peaks near zero. Preliminary tests (not shown here) demonstrated that the accuracy is not affected by
 188 small variations on these parameters. The final values used in this work were:

$$Q = 0.001^2 \times I_4 \quad R = \begin{bmatrix} 0.05^2 & 0 & 0 & 0 \\ 0 & 0.05^2 & 0 & 0 \\ 0 & 0 & 0.05^2 & 0 \\ 0 & 0 & 0 & 0.01^2 \end{bmatrix} \quad (7)$$

189 These values are approximated to those obtained by He et al., [27] for setting-up their Kalman
 190 filter. They applied an auto-regressive model to determine A (their final value was almost an identity
 191 matrix), Q , and R . In practice, all computations in both the computer (Matlab, Mathworks) and the
 192 embedded device are performed in bits and not in gravities to reduce the computational burden.

193 Figure 3 (Bottom panel) shows how state x_4 tends to a zero-bias sinusoidal shape when the person
 194 walks or jogs. This allows implementing a simple zero-crossing periodicity detector. Note how the
 195 periodicity is lost when the person trips and falls. The periodicity detector analyzes three seconds after
 196 a possible fall event. If during this 3 s window the periodicity is kept stable, we may expect that it was
 197 not a fall. The size of the window is selected as the minimum to guarantee that the person is slowly
 198 walking.

199 3.2. Feature extraction and classification

200 The feature extraction consists of a non-linear feature composed of two widely used ones, the
 201 sum vector magnitude and the standard deviation magnitude. The static sum vector magnitude is
 202 computed as the root-mean-square (RMS) of the static acceleration with previous bias removal:

$$J_1[k] = \text{RMS}(\vec{a}[k] - \vec{a}[k-1]) \quad (8)$$

203 where the bias is rejected with differentiation.

204 The standard deviation magnitude is computed at each time step k over a 1 s sliding window of
 205 the first three states of the Kalman filter: $\tilde{x}[k] = [\vec{x}[k-N], \dots, \vec{x}[k]] \in \mathfrak{R}^{3 \times N}$, where $N = 25$ is the size
 206 of the window (for a frequency sample of 25 Hz). This second feature is computed as follows:

$$J_2[k] = \text{RMS}(\text{std}(\tilde{x}[k])) \quad (9)$$

207 where $\text{std}(\cdot)$ is the standard deviation operator. The size of the window is selected as the one that
 208 includes the three stages of the fall: the pre-fall, the hit, and the time just after it [31]. Testing with
 209 windows between 0.25 and 2 s did not improve the accuracy, as expected [11].

210 The same sliding window can be used to determine the current bias on the y axis: $b_{ay}[k] =$
 211 $\text{mean}(\tilde{x}_y[k])$. Figure 4 shows both features with the jog-trip-fall example of Figure 3. The maximum
 212 values during jogging are half way of the fall in J_1 , but they get clearly distant in J_2 .

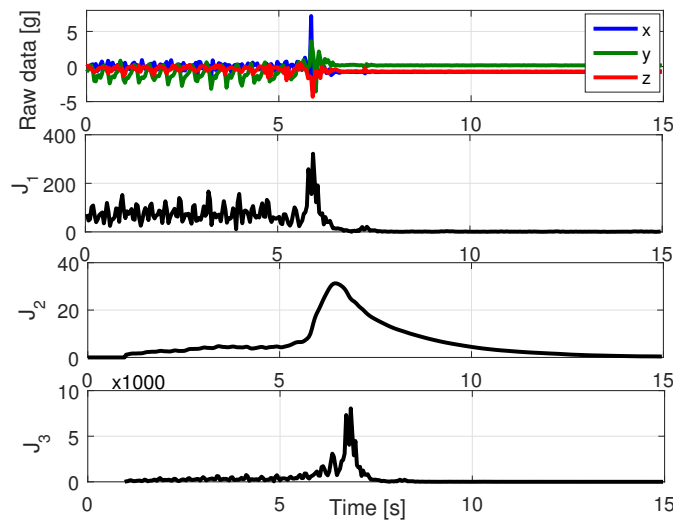


Figure 4. Feature extraction. (Top panel) Reference raw data (The subject is running, trips and falls). (Second panel) Feature J_1 detects the fall as a large difference between its peak and jogging peaks. (Third panel) Feature J_2 has a similar shape but with a larger percentual difference. Both J_1 and J_2 are computed in bits for reducing computations on the embedded device. (Bottom panel) J_3 is formed by J_1 and J_2 , increasing their coincidences and diminishing their differences.

213 Finally, the classification stage is performed over an indirect feature:

$$J_3[k] = \max(\tilde{J}_1[k]) \cdot \max(\tilde{J}_2[k])^2 \quad (10)$$

214 With $\tilde{J}_i[k] \in \mathcal{R}^{N \times 1}$ a sliding window with the last N values of the corresponding feature. This
 215 window is necessary as the Kalman filter takes some time to achieve the maximum, i.e., not always
 216 both metrics present a maximum at the same time. The objective of this product of features is to
 217 amplify the values of those activities where both features agree and to minimize those where both
 218 features disagree (see Figure 4, bottom panel). The square of J_2 prioritizes it over J_1 , as it is more
 219 accurate [11].

220 The classification consists of a single threshold over $J_3[k]$ computed at each time step k . The value
 221 of the threshold is defined after a training process. The robustness of the threshold was analyzed
 222 with a cross-validation set-up. This analysis was performed guaranteeing the same proportion of falls
 223 and ADL in all groups (4510 files randomly divided in 10 groups). A 10-fold cross-validation was
 224 performed, each fold had 4059 files for training and 451 for validation. Each group was used in one
 225 round as validation data.

226 Considering that most falls used for training come from young adults, we have taken in
 227 consideration two facts observed in [11]: (i) The elderly adults show in average lower accelerations
 228 in both ADL and falls (this behavior was originally studied in [32]); and (ii) the elderly adult that
 229 simulated falls always tried harder than the young adults to avoid hitting when falling, which is what
 230 one would expect from someone having an accident. These two facts turn into one recommendation: if
 231 there is a range for selecting the threshold, the lower acceleration value should be selected to avoid
 232 false negatives.

233 Accuracy (ACC), Sensitivity (SEN), and specificity (SPE) were used as performance metrics. SEN
 234 and SPE were calculated as specified in [33]:

$$\text{SEN} = \frac{TP}{TP + FN} \quad \text{SPE} = \frac{TN}{TN + FP} \quad (11)$$

235 where TP is the number of falls correctly classified, FN accounts falls that the algorithm did not
 236 detect, TN numbers ADL correctly classified, and FP indicates false falls. The accuracy was calculated
 237 using Eq. (12):

$$ACC = \frac{SEN + SPE}{2} \quad (12)$$

238 This balanced computation of the accuracy is selected due to the large difference between the
 239 number of ADL and fall files.

240 4. Results

241 4.1. Fall detection

242 We initially tested the performance of the proposed algorithm without detecting periodic activities.
 243 Table 2 shows the validation results with SisFall dataset over a 10-fold cross-validation (451 files
 244 each). All subjects and activities available in the dataset were included in the cross validation. The
 245 low detection accuracy obtained with J_1 (around 86 %) would raise questions about its usefulness.
 246 However, note how J_3 is significantly higher than J_2 (99.3 % vs. 96.5 %), i.e., although J_1 is not a good
 247 metric, combined with J_2 , it improves the individual accuracy values.

Table 2. Test on SisFall dataset without periodicity detector.

	J_1	J_2	J_3
Sensitivity [%]	92.92 ±1.56	96.06 ±1.52	99.27 ±0.78
Specificity [%]	81.72 ±2.22	96.79 ±1.12	99.37 ±0.36
Accuracy [%]	86.14 ±1.36	96.50 ±0.84	99.33 ±0.28
Threshold	110.88 ±3.23	22.88 ±0.027	42628 ±511.59

248 Figure 5 shows an activity-by-activity analysis for the three metrics. The horizontal red line is the
 249 threshold for the best accuracy value and the vertical red line divides ADL and falls. By comparing J_1
 250 (Figure 5(a)) and J_2 (Figure 5(b)), we observe that J_1 largely fails in periodic ADL (D03, D04, D06, D18,
 251 and D19) while J_2 does not, and J_2 goes closer to the threshold in activities where J_1 does not (D16
 252 for example). This separation was the basis to create J_3 ; it combines their results with a product but
 253 giving priority to J_2 (computed with square), given that it is more accurate. The small box in Figure 5(c)
 254 shows how all activities are more separated from the threshold and, more important, less fall files
 255 crossed the threshold (false negatives). This initial result significantly improves those obtained with
 256 previous approaches tested in [11] (none of them achieved more than 96 %).

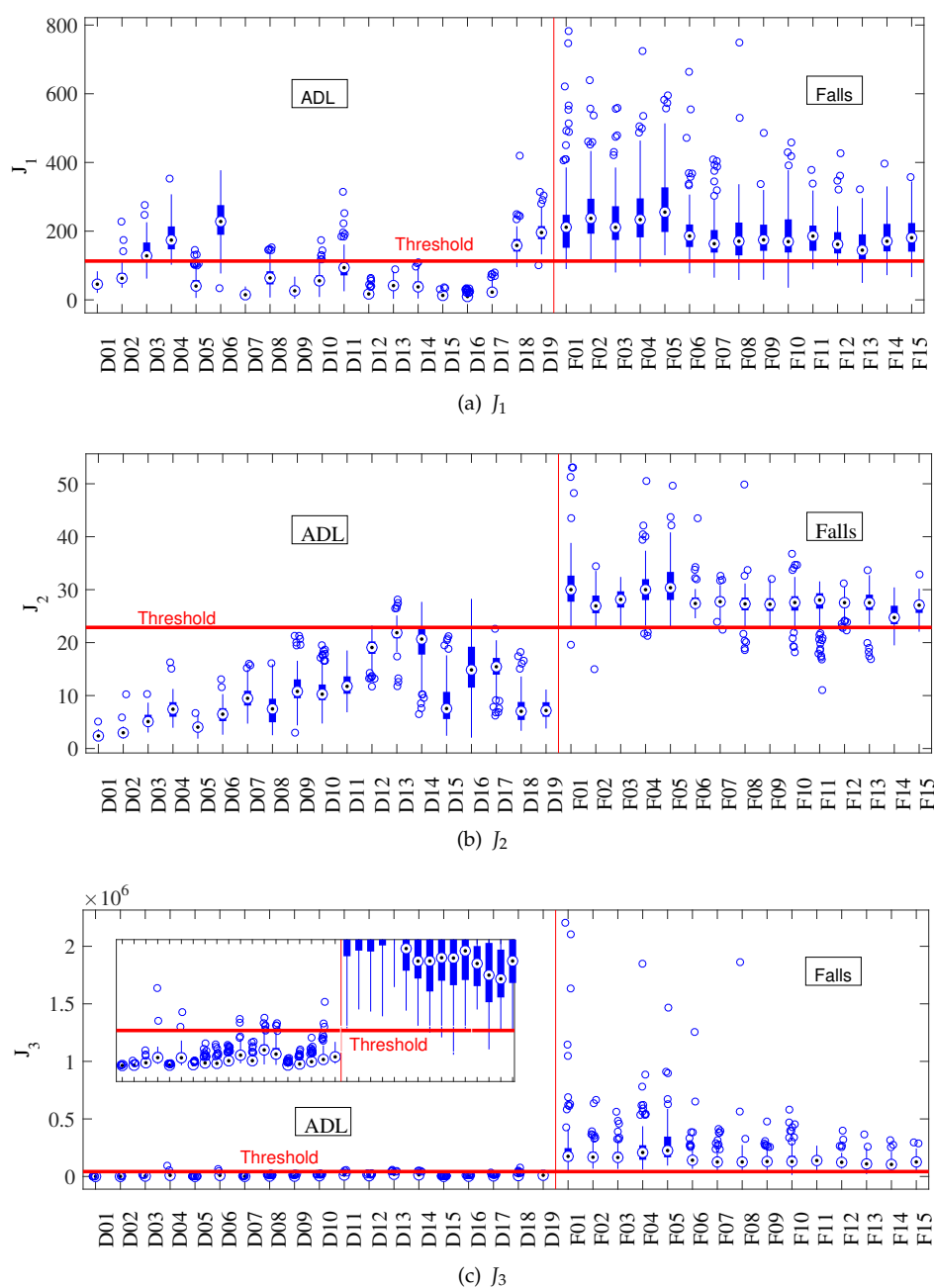


Figure 5. Individual activity analysis of the proposed algorithm tested with SisFall. The horizontal red line corresponds to the optimal threshold value, and the vertical one separates ADL and falls. (a) J_1 has large errors on periodic activities, while (b) J_2 fails in those that change the body angle. (c) They provide to J_3 a better discriminant capability (the small box at the left shows a vertical zoom).

257 We performed an additional test without including the Kalman filter in order to determine its
 258 effect on the algorithm. As expected, the accuracy of all metrics was significantly reduced: 82.65 % for
 259 J_1 , 91.03 % for J_2 , and 83.73 % for J_3 . However, this is not a fair comparison. The Kalman filter could
 260 be replaced by a set of band-pass filters and similar results should be obtained. But this strategy could
 261 severely affect the computational effort of the embedded device and its battery consumption.

262 4.2. Fall detection with periodicity detector

263 We then performed the same analysis but including the periodicity detector. The main purpose
 264 of this detector is to take J_1 to zero if a periodic activity is observed after a possible fall (false
 265 positive) –Same result is obtained if J_2 is selected. Table 3 shows the validation results after a 10-fold
 266 cross-validation. Compared to the previous analysis, J_1 has 8 % of improvement (94.32 %). Although
 267 one would expect a similar improvement in J_3 , this is not the case (although it is higher, with 99.4 % of
 268 accuracy) provided that on SisFall dataset, walk and jog only have one file per subject. Nevertheless,
 269 the periodicity detector was active in 606 files (13.5 % of the dataset).

270 Every dataset has a limited number of repetitions per activity. SisFall for example contains only
 271 one 1 minute repetition of walk per subject. However, it is expected that a walk will last more than one
 272 minute, i.e., the possibility of failure is higher with activities that the subject performs regularly (such
 273 as walking). Additionally, Figure 6 shows how the possibility of errors in other activities is lower due
 274 to their larger distance from the threshold.

Table 3. Test on SisFall dataset with periodicity detector.

	J_1	J_2	J_3
Sensitivity [%]	97.35 ±1.37	96.15 ±1.59	99.28 ±0.59
Specificity [%]	91.49 ±1.74	96.69 ±1.30	99.51 ±0.48
Accuracy [%]	94.42 ±1.33	96.42 ±0.58	99.39 ±0.36
Threshold	103.03 ±0.02	22.914 ±0.11	42230 ±985.01

275 Figure 6 shows the same individual activity analysis of Figure 5 but with the periodicity detector
 276 in J_1 . Figure 6 shows how activities D01 to D04 were turned to zero, as the detector confirmed that the
 277 subject was walking or jogging. In this case, J_3 shows more distance from the threshold than on the
 278 previous test (the threshold is updated accordingly). This indicates that even the cross-validation did
 279 not show a significant improvement on accuracy, the inclusion of the periodicity detector increased the
 280 robustness of the algorithm. Importantly, none fall was turned to zero in Figure 6, indicating that the
 281 periodicity detector was turned off in all periodic activities that finished in a fall.

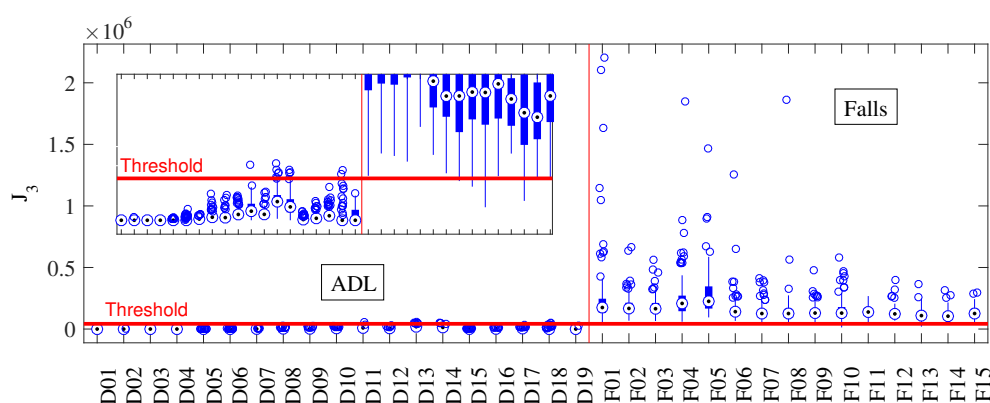


Figure 6. Individual activity analysis of the proposed algorithm including the periodicity detector. The horizontal red line corresponds to the optimal threshold value, and the vertical red line separates ADL and Falls. J_3 was turned to zero in all periodic ADL, this allowed it to increase the distance between most ADL and Falls.

282 4.3. On-line validation

283 In order to verify the off-line results presented in Table 3, we repeated the activities of SisFall with
 284 six young adults and an elderly person with the algorithm implemented on the device (see Section 2).
 285 During the tests, we verified on-line if the alarm was turned on (with an indicator incorporated to

286 the device). Additionally, all raw data and the device computations were recorded in text files. We
287 obtained no significant differences between the device and the computer. The proposed approach was
288 implemented on the embedded device with the same parameters and sample frequency defined above
289 (25 Hz). The threshold for J_3 was set at 40,000. The six volunteers performed 18 types of ADL and 15
290 types of fall in the same way that SisFall dataset was acquired (around 100 total trials per subject).

291 The participants presented a total of 4 false positives and 1 false negative. Subject SE06 (the elderly
292 person) did not show errors. All false positives were in D13 and D14 (bed related ones). Following
293 Figure 6, it is clear that these activities are commonly close to the threshold. A deeper analysis of this
294 problem (which is not reflected in the following test) demonstrated that when a person moves on the
295 bed, it is usual to separate the hip from the mattress and let it fall in the new position. The pad used for
296 this experiment is harder than a mattress increasing the false positive probability. The overall results
297 coincided with the statistics expected from Table 3.

298 4.4. Full-day (pilot) tests

299 We invited three independent elderly participants that were not part of SisFall acquisition (in
300 order to avoid biases) to carry the device for full days (see Section 2). We asked them to behave
301 normally while carrying the device during the day, and we checked the integrity of the devices every
302 couple of hours. They used the device permanently except during night sleep and shower. The files
303 were cut in segments to avoid computational overloads (one hour of recording implied a text file of
304 approx. 10 MB). This is a summary of the recorded activities:

- 305 • SM01: She assisted to Tae-Bo dancing lessons for adults (INDER Medellín, Colombia), and stayed
306 at home cooking, washing clothes, cleaning, and resting. She also made several trips to downtown,
307 walked on the street, and traveled by motorcycle.
- 308 • SM02: She stayed most of the time cooking at home, cleaning, and sitting on the dining room. She
309 is a dressmaker, so she stays long periods sit at home. She also made some trips by bus; and the
310 last two days she was sick resting at home.
- 311 • SM03: He did some trips to a business downtown and to a church. The rest of the time, he stayed
312 at home on bed or in the dining room (reading). In Figure 7 we show one of his trips downtown
313 (file SM03_1 of [34]). This trip included stairs, two train trips, and two bus trips. Note that despite
314 the wide amount of activities, the levels of feature J_3 were not close to the threshold (40,000).

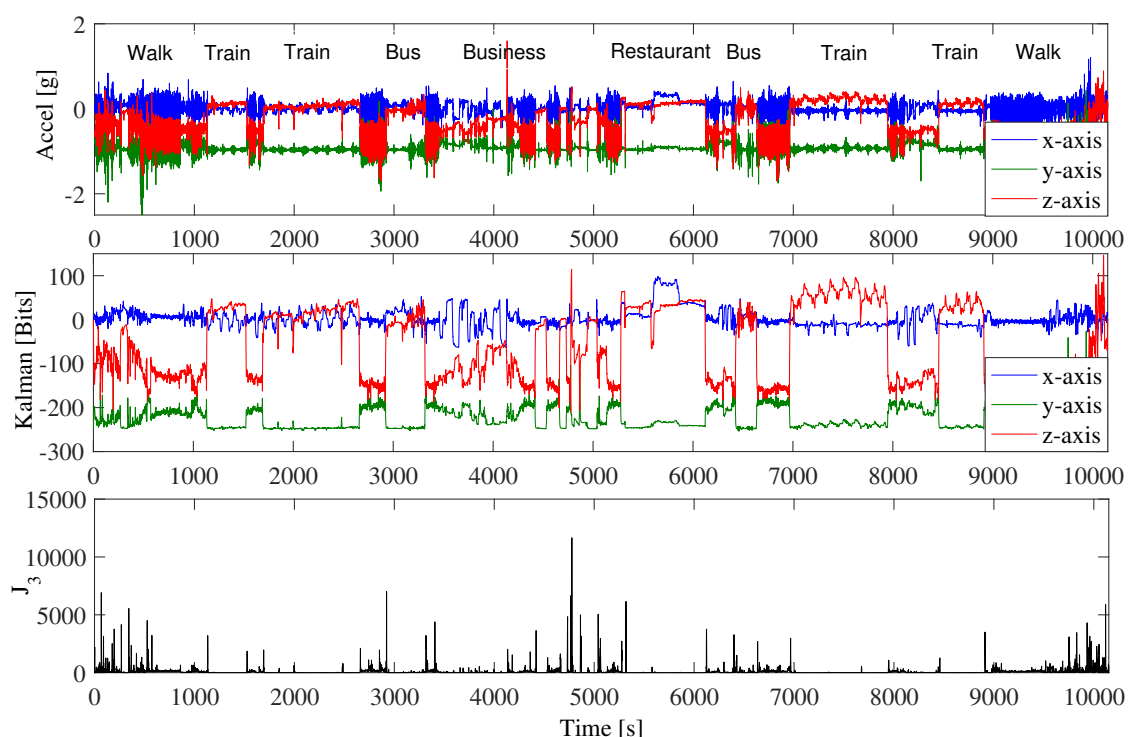


Figure 7. Trip to the downtown of subject SM03. (Top panel) Raw acceleration data, 2 hours and 45 minutes of recording. (Second panel) First three states of the Kalman filter. (Third panel) feature J_3 . It was always below the threshold (set at 40,000). Data recorded and processed with the embedded device of Figure 1.

315 We recorded approx. 170 hours of uncontrolled ADL divided in 77 text files. This dataset is
 316 available for download [34]. It includes raw acceleration data, low-pass filtered data, the states of the
 317 Kalman filter, the three classification features (J_1 , J_2 , and J_3), and an indicator of falls detected. These
 318 data were recorded with three embedded devices. We additionally released a binnacle of the activities
 319 performed by the participants and our explanation for every false positive.

320 The behavior of our devices is presented as follows:

- 321 • SM01: She had nine false positives during the recordings. Four of them were generated when
 322 standing up from a low chair or from the sidewalk. As shown in Figure 8(a), she used to stand up
 323 fast and her acceleration was close to the threshold. Another two false positives were generated
 324 when going downstairs (see Figure 8(b)). And the final three false positives were undetermined
 325 (presumably by direct hits to the device).

326 The subject is an active person and overall, her movements showed accelerations close (and
 327 sometimes higher) to young adults. This behavior contradicts findings of [32]. Our finding
 328 suggest that independent elderly people may show the same accelerations for ADL than young
 329 adults. Consequently, simulating with young people could be more feasible to compare with
 330 uncontrolled ADL of elderly people than simulating ADL with elderly people, who always
 331 showed lower acceleration values.

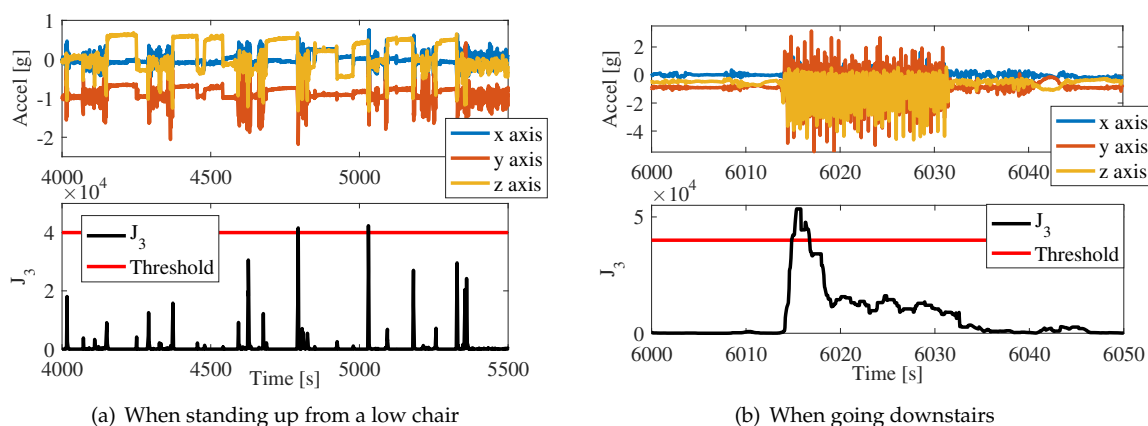


Figure 8. False positives. Subject SM01 showed high accelerations for everyday activities. (a) Note that her accelerations when standing up from a low chair just crossed the threshold. (b) The periodicity detector did not work correctly when going downstairs because the subject suddenly started the activity and the Kalman filter requires a few steps to compute the period.

- 332 • SM02: She had a total of seven false positives. One was a false positive for sitting fast on a chair.
- 333 Other five false positives were generated because she usually supported her belly against the
- 334 kitchen or the table. She went out of her home several times, unfortunately in two of them the
- 335 device got hits and lost the SD card. This is worrying as after an interview, we concluded that
- 336 she strongly hit the device in both cases presumably against furniture. We presume that it was
- 337 caused by her low height and by the shape of her belly (See Figure 1(b)). In order to solve this
- 338 issue, we asked her to use the device on the inner side of the belt (i.e., z-axis pointing towards
- 339 the back of the subject). After this modification she did not have more false positives.
- 340 • SM03: The subject did not have false positives.

341 In total, there were 16 false positives on this validation test (divided in two subjects). It is
 342 interesting that the number of false positives goes down with age. Indeed, when we changed the
 343 direction of the device of SM02, she did not present more false alarms. If we consider all falls, this
 344 means approximately one false alarm every 10 hours. This is a high value, but it would be reduced
 345 with some adjustments: (i) As shown in Figure 8(a), we could slightly increase the threshold after
 346 some training for highly active elderly subjects. (ii) Once we put the device of SM02 on the inner
 347 side of the belt, she stopped hitting it against furniture. She also used the device slightly to the
 348 right, we cannot determine the effect on the performance in case of a fall, but the data does not show
 349 significant differences on ADL. (iii) None of the subjects presented false positives during trips (even
 350 when traveling by motorcycle). We consider that this is a good measure of performance. Finally, false
 351 alarms at the very beginning or ending of the files were not considered for analysis. They were caused
 352 by devices turned on a direction different to vertical, or by taking the device off the belt before turning
 353 it off.

354 5. Discussion and Conclusions

355 In this paper, we presented a fall detection methodology with the following features: Simple
 356 frequency filtering, a non-linear feature based on commonly used ones, threshold-based classification,
 357 and a periodicity detector to avoid false positives. With these features, we generated a novel fall
 358 detection algorithm centered on a Kalman filter stage and a non-linear classification feature. The
 359 Kalman filter is not computationally intensive as it is Markovian and it demonstrated to be stable with
 360 acceleration data. We selected the Kalman filter because of its low computational cost and robustness;
 361 it provided an orientation level to a variance feature and at the same time a sinusoidal signal when
 362 the subject performed a periodic activity. This last result highly reduced the computational cost to

363 obtain the period of the signal, as it avoids to compute more elaborated approaches such as Wavelets
364 or auto-correlation [19].

365 The most significant improvement of this approach is the way how a combined non-linear feature
366 (J_3) provided higher accuracy (99.4 % with SisFall dataset) than the individual features (94.3 % and
367 96.4 %, respectively). We obtained this feature after analyzing individually several features with each
368 activity (finally keeping J_1 and J_2). They were selected as they were highly complementary (each fails
369 in different activities). The new non-linear feature used for this work was obtained in an intuitive way
370 and together with a threshold based classifier achieved 99.4 % of accuracy with SisFall dataset.

371 We implemented this methodology in embedded devices and tested it by redoing on-line all
372 SisFall activities. Then, we validated our work with full-day tests with the target population (two
373 female and one male, all over 60 years old). We asked them to do what they used to do, including
374 traveling by train and bus, doing exercise and cooking or cleaning. The devices behaved as expected;
375 with some false positives due to going downstairs, standing up from a low chair, and by direct hits to
376 the device. This final cause of false positives is out of the scope of this work and a good starting point
377 for a future analysis.

378 This final validation demonstrated that the proposed methodology can be used in real-life with
379 target population. We recorded and released [34] more than 170 hours of ADL recording with the
380 target population under uncontrolled conditions. This is to our knowledge the largest validation
381 dataset used for a fall detection approach. However, only real falls that may occur at any moment will
382 show the real accuracy of our approach.

383 In terms of power consumption, we observed that the devices were able to work in average for
384 18 hours per charge when recording data. Without recording data, the battery lasted between four
385 and five days (with the device turned off when the subjects were night sleeping). It is not adequate to
386 compare these results with other works because of the lack of information and different conditions
387 (most works do not specify the battery characteristics for example). However, we consider that our
388 approach is energy efficient because: (i) Sampling at 25 Hz instead of the usual 50–100 Hz implies
389 to be active for less time. (ii) With respect to the number of sensors, the gyroscope for example
390 consumes several times the current of the accelerometer (hundreds of μA compared to tens of μA), i.e.
391 having only one triaxial accelerometer avoids extra consumption. Finally, (iii) the Kalman filter is not
392 computationally intensive, and using a threshold based classification is optimal in terms of computing
393 load. Compared with neural networks or support vector machines, our approach is significantly more
394 efficient [9].

395 **Acknowledgments:** This work was supported by project: “Plataforma tecnológica para los servicios de
396 teleasistencia, emergencias médicas, seguimiento y monitoreo permanente a los pacientes y apoyo a los programas
397 de promoción y prevención”, code “Ruta-N: FP44842-512C-2013”. A. Sucerquia thanks Instituto Tecnológico
398 Metropolitano –ITM for their support on this work.

399 **Author Contributions:** All authors conceived and designed the approach; A.S. performed the experiments; A.S.
400 and J.D.L. analyzed the results; and all authors read and approved the final manuscript.

401 **Conflicts of Interest:** The authors declare no conflict of interest.

402

- 403 1. Masdeu, J.; Sudarsky, L.; Wolfson, L. *Gait Disorders of Aging. Falls and Therapeutic Strategies.*; Lippincott
404 -Raven, Philadelphia, 1997.
- 405 2. Vellas, B.; Wayne, S.; Romero, L.; Baumgartner, R.; Garry, P. Fear of falling and restriction of mobility in
406 elderly fallers. *Age and Ageing* **1997**, *26*, 189–193.
- 407 3. Lord, S.; Sherrington, C.; Menz, H. *Falls in Older People: Risk Factors and Strategies for Prevention.*, 1st ed.;
408 Cambridge University Press, 2001.
- 409 4. Delbaere, K.; Crombez, G.; Vanderstraeten, G.; Willems, T.; Cambier, D. Fear-related avoidance of activities,
410 falls and physical frailty. A prospective community-based cohort study. *Age and Ageing* **2004**, *33*, 368–373.
- 411 5. Lord, S.; Ward, J.; Williams, P.; Anstey, K. An epidemiological study of falls in older community-dwelling
412 women: the Randwick falls and fractures study. *Australian Journal of Public Health* **1993**, *17*, 240–245.

- 413 6. Henao, G.M.; Curcio Borrero, C.L.; Gómez Montes, J.F. Consecuencias De Las Caídas En Ancianos
414 Institucionalizados. *Revista de la asociación Colombiana de Gerontología y Geriatria* **2009**, *23*, 1221–1233.
- 415 7. Igual, R.; Medrano, C.; Plaza, I. Challenges, issues and trends in fall detection systems. *BioMedical*
416 *Engineering OnLine* **2013**, *12*, 1–24.
- 417 8. Shany, T.; Redmond, S.J.; Narayanan, M.R.; Lovell, N.H. Sensors-Based Wearable Systems for Monitoring
418 of Human Movement and Falls. *IEEE Sensors Journal* **2012**, *12*, 658 – 670.
- 419 9. Pannurat, N.; Thiemjarus, S.; Nantajeewarawat, E. Automatic fall monitoring: A review. *Sensors* **2014**,
420 *14*, 12900–12936.
- 421 10. Habib, M.A.; Mohktar, M.S.; Kamaruzzaman, S.B.; Lim, K.S.; Pin, T.M.; Ibrahim, F. Smartphone-Based
422 Solutions for Fall Detection and Prevention: Challenges and Open Issues. *Sensors* **2014**, *14*, 7181–7208.
- 423 11. Sucerquia, A.; López, J.; Vargas-Bonilla, F. SisFall: A fall and movement dataset. *Sensors* **2017**, *17*, 1–14.
- 424 12. Igual, R.; Medrano, C.; Plaza, I. A comparison of public datasets for acceleration-based fall detection.
425 *Medical Engineering and Physics* **2015**, *37*, 870–878.
- 426 13. Bagala, F.; Becker, C.; Cappello, A.; Chiari, L.; Aminian, K.; Hausdorff, J.M.; Zijlstra, W.; Klenk, J. Evaluation
427 of Accelerometer-Based Fall Detection Algorithms on Real-World Falls. *Plos one* **2012**, *7*, e37062.
- 428 14. López, J.D.; Ocampo, C.; Sucerquia, A.; Vargas-Bonilla, F. Analyzing multiple accelerometer configurations
429 to detect falls and motion. Latin American Congress on biomedical engineering, 2016.
- 430 15. Cola, G.; Avvenuti, M.; Vecchio, A.; Yang, G.Z.; Lo, B. An On-Node Processing Approach for Anomaly
431 Detection in Gait. *IEEE Sensors Journal* **2015**, *15*, 6640 – 6649.
- 432 16. Oner, M.; Pulcifer-Stump, J.A.; Seeling, P.; Kaya, T. Towards the Run and Walk Activity Classification
433 through Step Detection - An Android Application. 34th Annual International Conference of the IEEE
434 EMBS, 2012, pp. 1980 – 1983.
- 435 17. Wundersitz, D.W.T.; Gastin, P.B.; Richter, C.; Robertson, S.J.; Netto, K.J. Validity of a trunk-mounted
436 accelerometer to assess peak accelerations during walking, jogging and running. *European Journal of Sport*
437 *Science* **2014**, *2014*, 382–390.
- 438 18. Clements, C.M.; Buller, M.J.; Welles, A.P.; Tharion, W.J. Real Time Gait Pattern Classification from Chest
439 Worn Accelerometry During a Loaded Road March. 34th Annual International Conference of the IEEE
440 EMBS, 2012.
- 441 19. López, J.D.; Sucerquia, A.; Duque-Muñoz, L.; Vargas-Bonilla, F. Walk and jog characterization using a
442 triaxial accelerometer. IEEE International Conference on Ubiquitous Computing and Communications
443 (IUCC), 2015, pp. 1406–1410.
- 444 20. Kalman, R.E. A New Approach to Linear Filtering and Prediction Problems. *Transactions of the*
445 *ASME–Journal of Basic Engineering* **1960**, *82*, 35–45.
- 446 21. Bagalà, F.; Klenk, J.; Cappello, A.; Chiari, L.; Becker, C.; Lindemann, U. Quantitative Description of the
447 Lie-to-Sit-to-Stand-to-Walk Transfer by a Single Body-Fixed Sensor. *IEEE Transactions on Neural Systems*
448 *and Rehabilitation Engineering* **2013**, *21*, 624–633.
- 449 22. Berg, K.; Wood-Dauphinee, S.; Williams, J.; Maki, B. Measuring balance in the elderly: validation of an
450 instrument. *Canadian Journal of Public Health* **1992**, *83*.
- 451 23. Otebolaku, A.M.; Andrade, M.T. User context recognition using smartphone sensors and classification
452 models. *Journal of Network and Computer Applications* **2016**, *66*, 33–51.
- 453 24. Novak, D.; Rebersek, P.; De Rossi, S.M.M.; Donati, M.; Podobnika, J.; Beravs, T.; Lenzi, T.; Vitiello, N.;
454 Carrozza, M.C.; Muniha, M. Automated detection of gait initiation and termination using wearable sensors.
455 *Medical Engineering & Physics* **2013**, *35*, 1713–1720.
- 456 25. Yuan, X.; Yu, S.; Dan, Q.; Wang, G.; Liu, S. Fall Detection Analysis with Wearable MEMS-based Sensors.
457 16th International Conference on Electronic Packaging Technology (ICEPT), 2015, pp. 1184–1187.
- 458 26. Li, H.; li Yang, Y. Research of elderly fall detection based on dynamic time warping algorithm. Proceedings
459 of the 35th Chinese Control Conference, 2016.
- 460 27. He, J.; Bai, S.; Wang, X. An Unobtrusive Fall Detection and Alerting System Based on Kalman Filter and
461 Bayes Network Classifier. *Sensors* **2017**, *17*, 17.
- 462 28. Mao, A.; Ma, X.; He, Y.; Luo, J. Highly Portable, Sensor-Based System for Human Fall Monitoring. *Sensors*
463 **2017**, *17*, 15.
- 464 29. Zhang, C.; Lai, C.F.; Lai, Y.H.; Wu, Z.W.; Chao, H.C. An inferential real-time falling posture reconstruction
465 for Internet of healthcare things. *Journal of Network and Computer Applications* **2017**, *89*, 86–95.

- 466 30. Luenberger, D. An Introduction to Observers. *IEEE Transactions on Automatic Control* **1971**, *16*(6), 596–602.
- 467 31. Noury, N.; Rumeau, P.; Bourke, A.; ÓLaighin, G.; Lundy, J. A proposal for the classification and evaluation
468 of fall detectors. *IRBM* **2008**, *29*, 340–349.
- 469 32. Klenk, J.; Becker, C.; Lieken, F.; Nicolai, S.; Maetzler, W.; Alt, W.; Zijlstra, W.; Hausdorff, J.; van Lummel, R.;
470 Chiari, L.; Lindemann, U. Comparison of acceleration signals of simulated and real-world backward falls.
471 *Medical Engineering and Physics* **2011**, *33*, 368–373.
- 472 33. Noury, N.; Fleury, A.; Rumeau, P.; Bourke, A.; Laighin, G.; Rialle, V.; Lundy, J. Fall detection – Principles
473 and Methods. 29th Annual International Conference of the IEEE EMBS, 2007, pp. 1663 – 1666.
- 474 34. Sisfall 2: Real-life/real-time elderly ADL. <http://sistemic.udea.edu.co/en/investigacion/proyectos/english-falls/>,
475 2018.